Theoret. chim. Acta (Berl.) 11, 145—155 (1968)

The Electronic Structures of Pyridine-N-Oxide and Related Compounds

E. M. EVLETH

Centre de Mécanique Ondulatoire Appliquée, Paris, France
and
The University of California, Santa Cruz, California 95060*

Received April 3, 1968

The electronic structures of pyridine *n*-oxide, 2- and 4-methoxypyridine *n*-oxide, their conjugate acids, and 2- and 4-pyridone are calculated using the Pariser-Parr-Pople SCF-CI approximation. The results indicate that the $^1B_1 \leftarrow {}^1A_1$ transition of pyridine *n*-oxide lies in the same energy region as the transition previously assigned as being $n-\pi^*$. The strong electronic transitions in the 250–280 mμ region of pyridine-*n*-oxide, 4-methoxypyridine *n*-oxide, and 4-pyridone are assigned as being $^1A_1 \leftarrow {}^1A_1$.

Die elektronischen Strukturen von Pyridin-N-Oxyd, 2- und 4-Methoxypyridin-N-Oxyd, ihrer Kationen, und von 2- und 4-Pyridon wurden nach der Methode von Pariser-Parr-Popple SCF-CI berechnet. Es ergibt sich, daß der $^1B_1 \leftarrow {}^1A_1$ Übergang des Pyridin-N-Oxyds etwa die gleiche Energie besitzt, wie die bisher einem $n-\pi^*$ Übergang zugeordnete Bande. Der intensitätsstarke Übergang des Pyridin-N-oxyds, 4-Methoxypyridin-N-oxyds und 4-Pyridons im Bereich von 250–280 mμ wird einem $^1A_1 \leftarrow {}^1A_1$ Übergang zugeordnet.

Les structures électroniques de l'oxyde de pyridine, des *n*-oxydes de 2- et 4-methoxypyridine, leurs cations, et les 2- et 4-pyridone sont calculés par l'approximation Pariser-Parr-Pople SCF-CI. Les résultats obtenus indiquent que la transition $^1B_1 \leftarrow {}^1A_1$ du *n*-oxyde de pyridine est située dans la même région d'énergie que la transition assignée auparavant comme étant $n-\pi^*$. Les transitions électroniques fortes dans la région de 250–280 mμ du *n*-oxyde de pyridine, du *n*-oxyde de 4-methoxypyridine et du 4-pyridone sont assignées comme étant $^1A_1 \leftarrow {}^1A_1$.

Introduction

Three electronic transitions have been reported for pyridine-*n*-oxide [1–5]. The principle transition lies in the 280 mμ region (hexane) with a moderately strong intensity ($\varepsilon = 10{,}000$, $f = 0.173$) [3]. A weaker band is observed in non-polar solvents [3] in the region of 320 mμ ($\varepsilon = 3000$, $f = 0.012$). A third transition occurs in the 215 mμ region [3] also having a moderately strong intensity ($\varepsilon = 18{,}000$). The assignments of these transitions have varied. The 320 mμ transition was originally assigned as being $n-\pi^*$ [3, 4] on the basis of blue shift characteristics in polar solvents. This assignment was challenged by both Sidman [6] and Murrell [7] on the basis that: i) the intensity was too large for a $n-\pi^*$ transition, ii) the di-*n*-oxyde of azomethane exhibited no $n-\pi^*$ transition in this energy region, and iii) the major 280 mμ transition also exhibits blue shift characteristics in polar solvents and thus the 320 mμ transition could also be a $\pi-\pi^*$ charge transfer transition. The recent work of Ziolkowsky and Dörr [8] demonstrated that pyridine-*n*-oxide exhibited neither fluorescence nor phosphorescene. The polarized emission studies of other *n*-oxides did not indicate the presence of $n-\pi^*$ transitions.

---

* Present address.

The charge transfer calculations of Kubota [1, 2] assign the strong 280 mμ transition of pyridine *n*-oxyde as being ${}^1A_1 \leftarrow {}^1A_1$. Computationally, this transition is a mixture of ${}^1B_a$, ${}^1L_a$, and ${}^1A_1$ components but dominated by the latter charge transfer contribution. Kubota argues [2] that the intensity of the 320 mμ transition is not too high for a $n-\pi^*$ transition. Kubota does predict [1, 2] that a transition having a high contribution from the ${}^1L_b \leftarrow {}^1A_1$ component should exist in the same energy region as the stronger 280 mμ transition. Kubota assigns the 215 mμ transition as being largely a ${}^1L_a \leftarrow {}^1A_1$ transition.

The SCF–CI calculation of Saison and Jaffé [9] predicts two transitions in the 280 mμ region, the stronger of which is the ${}^1B_1 \leftarrow {}^1A_1$ transition, and the weaker ${}^1A_1 \leftarrow {}^1A_1$. The transition further in the UV region is assigned ${}^1A_1 \leftarrow {}^1A_1$. In addition, Jaffé has qualitatively assigned [4] the 280 mμ transition of amino and methyl substituted *n*-oxydes as being L_b transitions.

The conflicts in the above assignments warrant a more theoretically intense examination of the spectral features of pyridine *n*-oxide (I) and structurally related compounds. For this purpose we have choosen to examine the electronic structures of I, 2- and 4-methoxypyridine *n*-oxide (II and III), 2- and 4-pyridone (IV and V) and the zwitterion (VI) of 3-hydroxypyridine. The conjugate acids of I, II, and III (ICA, IICA, and IIICA) are also computed.

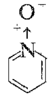
I

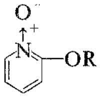
II


III

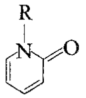
IV

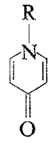
V

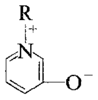
VI

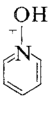
ICA

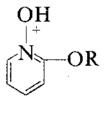
IICA

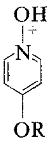
IIICA

Method of Calculation

The calculations presented here were obtained using the Bessis-Chalvet SCF-CI program. The standard π electron approximations of Pariser, Parr [10], and Pople [11] were utilized. The coulomb and resonance parameters utilized are listed in Tables 1 and 2. The electron repulsion integrals were calculated using

Table 1. *Coulomb and resonance parameters*

Atom	I_p^*	Z	$\langle 11 \mid 11 \rangle$[a]
N	28.16	4.25	15.92
C	11.22	3.25	10.53
O^-	17.17	4.55	14.30
O	35.50	4.90	21.55

I_p = valence state ionization potential, Z = Slater Z value, $\langle 11 \mid 11 \rangle$ = one centered repulsion integral.

---

[a] All energies given in electron volts.

the approximation of Parr [12]. Geometries were computed using the bond distances listed in Table 2. Since the six member rings are not symmetrically hexagonal with these interatomic distances, the ring geometries were computed by assuming approximately equal distortion to the internal bond angles. The oscillator strengths were estimated from the experimental molar extinction coefficient, ε_{max}, using the approximation of Sandorfy [13],

Table 2. *Bond distances and resonance parameters*

Bond	Type	Distance (Å)	Resonance parameter (eV)
$N^+–O^-$	n-oxide	1.27	−2.60
$N^+–O–H$	protonated	1.39	−2.60
N=C	pyridinium	1.39	−2.60
C=C	pyridinium	1.39	−2.40
C=C	pyridone	1.35	−2.40
C—N	pyridone	1.39	−2.45
C—C	pyridone	1.45	−2.20
C=O	pyridone	1.24	−2.60
$C–O^-$	oxy-pyridinium	1.39	−2.60

$$f_{est} = 4.32 \times 10^{-9} \times 1.06 \times \varepsilon_{max} \times h$$

where h is the band width (cm^{-1}) at one-half ε_{max}. A band width of 5000 cm^{-1} was assumed. These approximations represent an upper limit in the estimated value of f.

In this investigation the number of excited configurations incorporated in the CI treatment has been limited to 10 singly excited states. In two calculations 10 doubly excited configurations were also included.

Results and Discussion

A comparison of the computed and experimental spectral features of I, II, and III is shown in Table 3. Only the four lowest computed energy transitions are listed along with the oscillator strengths and symmetries of the states.

The experimental data has been reported in various solvents and it must be stressed that the spectra of these materials are strongly solvent dependent. In particular, the transition previously assigned as being $n-\pi^*$ in I is not observed in water [1, 2] or acetonitrile [14]. The strong 4.4 eV transition (heptane) of I [3] is shifted to 4.9 eV in water [1, 5].

The computed order of the symmetries of the π excited states of I and III are ${}^1B_1$, ${}^1A_1$, and ${}^1B_1$. In each case the lowest energy π transition, ${}^1B_1 \leftarrow {}^1A_1$ is computed to have the weakest intensity. The orders of relative experimental strengths of the computed intensities in I are the same. Only one strong transition is experimentally reported for III. Thus, within this analysis, the 4.0 eV transition in I, previously assigned [1–5] as being $n-\pi^*$, is possibly ${}^1B_1 \leftarrow {}^1A_1$. The experimental spectrum of II exhibits two well defined transitions of approximately the same intensity in the 4.0–5.0 eV region together with a much stronger transition in the 6 eV region. The calculated and experimental orders of the intensities of the transitions in II are in relative agreement. Additionally, it should be noted that substitution of methoxy on I has very little influence on the computed position of these transitions. The reason for this will be discussed later.

The assignments of the electronic transitions in I are opposite to those of Saison and Jaffé [9] and only in partial agreement with the charge transfer calculation of Kubota. The previous SCF-CI calculation [9] on I differed in several important respects from the one reported here. A principle parameter difference lies in the assigned value of the one centered electron repulsion integral for the oxygen. The value used here, 14.3 eV, is to be compared with a value of 14.127 eV used by Kubota [2], a value of 15.27 eV obtained from Hinze and Jaffé [16] and a value of 2.71 eV (?) used by the previous SCF-CI calculation. In addition Saison and Jaffé included doubly excited configurations and obtained a much higher computed transition dipole for the $^1B_1 \leftarrow {}^1A_1$ transition than for the $^1A_1 \leftarrow {}^1A_1$ (0.43 compared to 0.08). The problem of computed intensities in calculations incorporating doubly excited configurations is not yet theoretically resolved (vide infra).

Table 3. *Comparison of the computed and experimental spectra of structures I, II, and III*

Structure	State	Computed[a]			Experimental			
		E_t	f	Sym.	E_t	$\varepsilon_{\max}$	$f_{\text{exptl.}}$	$f_{\text{est.}}$
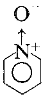	G	—	—	$^1A_1$				
	1	4.27	0.04	$^1B_1$	4.0^b	—	0.012^b	
	2	4.59	0.19	$^1A_1$	$4.4^{b,c}$	14,500	0.173^b	(0.33)
	3	6.17	0.44	$^1B_1$	$5.7^{b,c}$	18,100	—	(0.41)
	4	6.29	0.80	$^1A_1$	—	—	—	
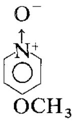	G	—	—	$^1A_1$				
	1	4.02	0.09	$^1B_1$	—	—		
	2	4.56	0.21	$^1A_1$	4.7^d	16,300		(0.37)
	3	6.19	0.19	$^1B_1$	—	—		
	4	6.29	0.50	$^1A_1$	—	—		
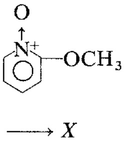	G	—	—	$\overset{\uparrow}{\underline{/a}}$				
	1	4.20	0.05	+55°	$4.2^{d,e}$	4,500		(0.10)
	2	4.45	0.11	+67°	5.0^e	7,600		(0.17)
	3	5.95	0.59	−10°	5.8^e	25,000		(0.57)
	4	6.16	0.82	+80°	—	—		

[a] E_t = Transition energy in electron volts, $\varepsilon_{\max}$ = molar extinction coefficient, Sym. = symmetry (C_{2v}) $\overset{\uparrow}{\underline{/a}}$ direction of the transition moment with respect to X axis, $f_{\text{est.}}$ = estimated oscillator strength (see text).

[b] In heptane, Ref. [3].

[c] 4.9 and 6.0 eV in water, Ref. [1, 4], 4.5 and 5.7 eV in acetonitrile, Ref. [14].

[d] In water, Ref. [15].

[e] 3.9, 4.6, and 5.5 eV, respectively, in acetonitrile, Ref. [14].

Conceptually, pyridine *n*-oxide is a perturbed substituted benzene. Both Stevenson [17] and Petruska [18] have been successful in interpreting the spectra of substituted benzenes within the framework of free electron theory. Both mildly and strongly substituted benzene exhibit spectral features which can be quantitatively and qualitatively labeled as arising from the ${}^1L_b \leftarrow {}^1A_1$ and ${}^1L_a \leftarrow {}^1A_1$ transitions in benzene [17, 18]. Characteristically, the former transition is weak and the latter strong. Generally the L_b transitions have values of ε in the region of 100–3,000 while the L_a transitions are in the region of 7,000 or over [17, 18, 19]. In polysubstituted benzenes, a limited number of cases have been observed in which neither transition is sufficiently weak or strong to be labeled L_a or L_b [17, 20]. However, within the above context, the strong transitions in the 280 mμ region for I and III are L_a. The non-observance of the L_b transition in III and questionable observance in I is not unique. The L_b transitions of a number of substituted benzenes have not been observed [17] due presumably to their near degeneracy with the stronger L_a transition [17–22]. This is generally true with donor-acceptor para-disubstitution. In the majority of cases the ortho and meta substitution of donar-acceptor pairs [17, 18, 20] yields materials whose spectral features exhibit stronger L_a transitions at higher energies than the weaker L_b transitions. Thus the qualitative expectation is that both I and III, having C_{2v} symmetry, will exhibit a strong ${}^1A_1 \leftarrow {}^1A_1$ transition, perturbationally related to the ${}^1L_a \leftarrow {}^1A_1$ transition in benzene. The weaker ${}^1B_1 \leftarrow {}^1A_1$ transition, perturbationally ${}^1L_b \leftarrow {}^1A_1$, will lie in the same energy region. If this qualitative analysis is correct, then the low symmetry of II will generate the appearance of two resolved transitions in the same energy region as the strong transitions I and III. This is in direct analogy to the ortho-disubstituted benzenes [17]. Qualitatively, the 1st and 2nd $\pi - \pi^*$ observed transitions in II are perturbationally related, respectively, to the L_b and L_a transitions in benzenes. It must be stated, however, that the strict labeling of the two lowest electronic transitions in perturbed benzenes as being L_b or L_a runs into semantic difficulty. The charge transfer calculations of Kubota on I indicate [1] that the total weight of the charge transfer component (80%) far exceeds the L_a component (8%) in the ${}^1A_1 \leftarrow {}^1A_1$ transition.

ICA, IICA, and IIICA

The experimental electronic transitions of ICA in the 4.8 and 5.7 eV region are both relatively weak and somewhat similar to 1-methyl pyridinium perchlorate (4.8 eV, $\varepsilon = 4{,}600$ [23], and 6.0 eV, $\varepsilon = 3{,}800$ [14]). Theoretical calculations on pyridine and pyridinium ion [25–27] indicate that the lowest $\pi - \pi^*$ electronic transitions are ${}^1B_1 \leftarrow {}^1A_1$, and are perturbationally related to the L_b transition in benzene. Table 4 shows a comparison of the computed and observed spectral features of ICA, IICA, and IIICA. The calculated positions of the 2nd electronic transitions in ICA and IICA do not match with the experimental values, the difference being in the order of 0.5–0.6 eV. The computed oscillator strengths of the 2nd transition are much lower than experimental. Previous theoretical calculations on pyridinium ion [24, 25] indicate a strong parameter dependence of the oscillator strength of the ${}^1A_1 \leftarrow {}^1A_1$ transition.

Only a single strong transition is reported for IIICA [15]. Qualitatively, the strong intensity of this transition indicates that it has considerable charge transfer character along the symmetry axis of the molecule and is assigned as being ${}^1A_1 \leftarrow {}^1A_1$. This is in agreement with the calculation. In analogy with the cases discussed previously the weaker ${}^1B_1 \leftarrow {}^1A_1$ transition of IIICA is nearly degenerate to and covered by the ${}^1A_1 \leftarrow {}^1A_1$ transition.

Table 4. *Comparison of the computed and experimental spectra of the protonated species of I, II, and III*

Structure	State	Calculated[a]			Experimental		
		E_t (eV)	f	Sym.	E_t (eV)	ε	$f_{\text{est.}}$
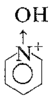	G			$^1A_1$			
	1	4.73	0.09	$^1B_1$	4.8[b]	2,900	0.07
	2	5.19	0.02	$^1A_1$	5.7	4,900	0.11
	3	6.85	0.92	$^1B_1$	–	–	–
ICA	4	6.95	1.13	$^1A_1$	–	–	–
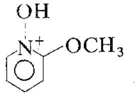	G			$\measuredangle a$			
	1	4.57	0.18	$-7°$	4.4[c]	6,300	0.15
	2	5.16	0.006	$+28°$	5.9	5,200	0.12
	3	6.74	1.19	$+63°$	–	–	–
IICA $\longrightarrow X$	4	6.88	0.81	$-31°$	–	–	–
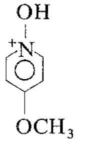	G			$^1A_1$			
	1	4.70	0.007	$^1B_1$	–	–	–
	2	5.00	0.10	$^1A_1$	5.1[c]	12,000	0.28
	3	6.30	0.77	$^1B_1$	–	–	–
	4	6.89	1.23	$^1A_1$	–	–	–
IIICA							

[a] E_t = transition energy, Sym. = symmetry, ε = molar extinction coefficient, $f_{\text{est.}}$ = estimated oscillator strength. $\measuredangle a$, transition moment with respect to X axis.

[b] Ref. [5], in water.

[c] Ref. [15], in water.

IV, V, and VI

Using benzyl anion as a model, Mason [28] has applied simple perturbation theory to the analysis of the spectral features of a number of the cationic, anionic, and neutral species of 2-, 3-, and 4-hydroxypyridine. This includes the compounds IV, V, and VI. Mason's analysis [28][1] indicates that the 4.2 and 5.5 eV transitions in IV and the 3.9 and 5.0 eV transitions in VI are perturbationally related to the $^1B_1 \leftarrow {}^1A_1$ and $^1A_1 \leftarrow {}^1A_1$ transitions, respectively, in benzyl anion. The 4.8 eV transition in V is assigned [28] as being $^1A_1 \leftarrow {}^1A_1$ with a weaker (unobserved) $^1B_1 \leftarrow {}^1A_1$ transition in the same energy region. The calculations shown in Table 4 are in essential agreement with Mason's analysis.

Effect of Configuration Interaction

Shown in Table 5 is the effect of the inclusion of a limited number (10) doubly excited configurations on the calculations for IV and V. Within the context of the limited CI treatment used here, the inclusion of doubly excited configurations has a mild effect on narrowing the computed separation between the two lowest electronic transitions and a strong effect in lowering the computed oscillator strength of some transitions. In this respect the effect of inclusion of doubly excited configurations is similar to what has been previously reported by Allinger and co-workers [30–32] and Evleth [33, 34]. In particular, Allinger and Stuart [32] have recently shown the computational importance of the inclusion of a large

---

[1] The analysis of Mason is strengthened by the linear relationship [29] between the observed and calculated transition energies of these species.

Table 5. *Comparison of the computed and experimental spectra of structures IV, V, and VI*

Structure	State	Computed[a]			Computed				%*DE*	Experimental			
		E_t	f	Sym.	E_t^b	f	$E_t^{b,c}$	f		E_t^d	ε_{max}^d	$f_{\text{exptl.}}$	$f_{\text{est.}}$
V 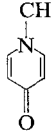	G			$^1A_1$					2				
	1	4.24	0.04	$^1B_1$	4.28	0.05	4.62	0.05	1	—	—	—	—
	2	5.01	0.41	$^1A_1$	5.05	0.38	4.80	0.26	19	4.8	18,900	0.328	(0.43)
	3	6.13	0.19	$^1B_1$	6.23	0.19	6.27	0.01	36	—	—	—	—
	4	6.85	1.14	$^1A_1$	6.87	1.13	6.50	0.17	—	—	—	—	—
IV 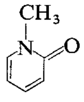	G			$\underline{\overset{\uparrow}{l}a}$					2				
	1	4.22	0.25	−28°	4.37	0.22	4.51	0.20	4	4.2	5,700	0.11	(0.13)
	2	5.40	0.19	+45°	5.36	0.20	5.03	0.09	13	5.5	6,100	—	(0.14)
	3	6.74	1.02	+48°	6.71	0.96	6.43	0.45	21	—	—	—	—
	4	6.91	0.00	+30°	6.91	0.04	6.74	0.13	20	—	—	—	—
VI 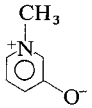	G			$\underline{\overset{\uparrow}{l}a}$									
	1	2.75	0.14	+35°						3.9	5,800	0.088	(0.13)
	2	4.46	0.22	−29°						5.0	8,100	—	(0.19)
	3	5.70	0.39	−15°						—	—	—	—
	4	6.64	0.83	−43°						—	—	—	—
$\xleftrightarrow{X}$													

---

[a] Parameters from Table 1, E_t = Transition energy in eV, f = oscillator strength, $\underline{\overset{\uparrow}{l}a}$, transition moment with respect to X axis.

[b] Resonance parameters same as Table 1, with exception that $\Theta_{C-C} = -1.90$ eV.

[c] 10 doubly excited configurations included, %*DE* = sum of the total percent weight of doubly excited configurations in configurational wave function.

[d] Ref. [28], in water.

number of singly, doubly, and higher configurations. Unfortunately such inclusions generate a large diminution in the computed oscillator strength. The utilization of computational methods for the analysis of the observed spectral features of a molecule becomes difficult when observed strong transitions are to be matched with those computed to be weak. It is standard to regard oscillator strength calculations as slightly better than order of magnitude estimates. The results of Allinger and Stuart [32] indicate that for the 3rd electronic transition of styrene the oscillator strength is reduced from 0.5 to 0.004 on the massive inclusion of higher configurations. Such results bring into suspect all previous computational assignments of the upper electronic transitions in large molecular systems. Within the context of the results presented here faith can only be placed on the assignments of the lowest two π electronic transitions.

Electronic Densities, Solvent Spectral Effects, and Substituent Effects

Shown below are the computed electron densities of the ground and excited states of I, I CA, III and V. A comparison of the computed π electron dipole moment with the experimental values if shown in Table 6.

Table 6. *Comparison of the computed and experimental dipole moments*

Structure	Calculated	Experimental	Ref.
I	4.76	4.18	[38]
II	4.43		
III	6.20	5.08	[35]
IV	4.12	4.15	[37]
V	6.32	6.9	[37]

The computed dipole moments of I, IV and V approximate those already estimated by the modified Hückel method (Omega Treatment) [38]. As shown by Clementi [39] in the case of pyrrole, π electron calculations approximate the π dipole moment but that the experimental dipole moment is dominated by sigma bond effects. Generally, it will be difficult to compare π electron dipole moments with experimental value when small moments are observed. Substitutent effects on π electron transitions indicate that changes in electronic charge distribution between the ground and excited states can be dominated by π electron contributions [20].

The polar solvent-blue shift characteristics of pyridine n-oxide (I) have been shown by Kosower [40] to be linearly and strongly dependent of the Z value of the solvent. Kosower's results indicate that the dipole moment of pyridine n-oxide should decrease and perhaps be reversed in the excited state corresponding to the $^1A_1 \leftarrow {}^1A_1$ transition.

The calculation indicate that the dipole moments of the $^1B_1$ and $^1A_1$ excited states (0.66 and 1.33, respectively) are in a direction opposite to the computed ground state value of 4.76 D. Both transitions are predicted to have nearly the same solvent characteristics. The computed electron distributions of both states indicate nearly the same degree of transfer of electronic charge from the oxygen to the ring. In this sense both transitions can be considered as having a considerable amount of charge transfer contribution. This result also counters the previous

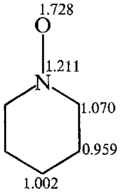

$\mu_{\text{calcd.}} = -4.76$
(Debyes) Ground ($^1A_1$)
State

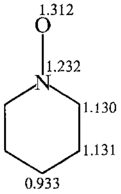

$+0.66$
1st ($^1B_1$)
Excited

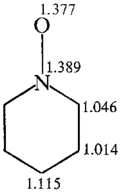

$+1.33$
2nd ($^1A_1$)
States

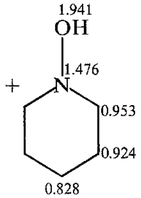

Ground ($^1A_1$)
State

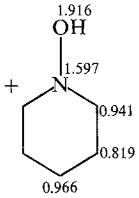

1st ($^1B_1$)
Excited

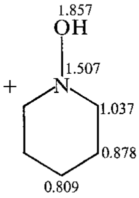

2nd ($^1A_1$)
States

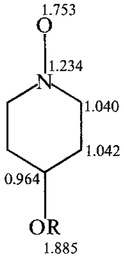

Ground ($^1A_1$)
State

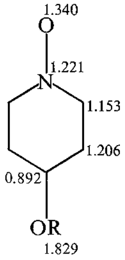

1st ($^1B_1$)
Excited

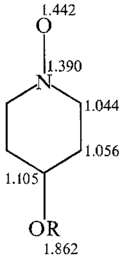

2nd ($^1A_1$)
States

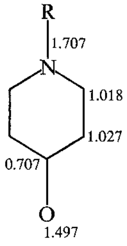

$\mu_{\text{calcd.}} = -6.32$
Ground ($^1A_1$)
State

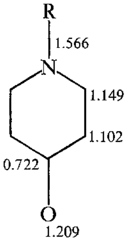

-3.2
1st ($^1B_1$)
Excited

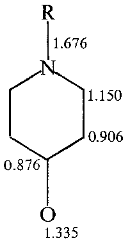

-3.7
2nd ($^1\mathrm{A}_1$)
States

$n \rightarrow \pi^*$[3] assignment of the 320 mμ transition in I on the basis of blue shift characteristics.

The effect of methoxy-substitution on the spectra of I can be rationalized within the context of the observed electronic charge distribution in the ground and $^1B_1$ and $^1A_1$ excited states of I [20]. First, in contrast with pyridinium, the ring system in the ground state of I represents an electron rich system. It is *even more so* in the excited states of I. Thus the effect of substitution on the positions of the L_b and L_a transitions of I are analogous to phenoxide ion [17] and in contrast to the effects in nitrobenzene [17, 21] or benzenediazonium cation [20]. Massive red shifts of 0.7–0.8 eV are observed for the L_a transitions of nitrobenzene [17] and benzenediazonium cation [20] with the substitution of methoxy in the para position. The corresponding shift in the L_a transition in going from I to III is about 0.2 eV (in water). Similarly, it is qualitatively predicted that the L_b and L_a transitions of II are essentially unshifted from the corresponding values in I.

The polar solvent-blue shift characteristics of 1-methyl-4-pyridone (V) are weaker [28] than with I. The ground state and excited state dipole moment calculations indicate that V undergoes a decrease in dipole moment on excitation. However, the change in dipole moment between the ground and excited states of V is neither reversed nor as great in magnitude as with I.

As pointed out previously [28, 41] it is *not possible* to rationalize the charge distribution of the excited states with the use of limited number of valence bond structures (Va and Vb). On excitation both the nitrogen and oxygen atoms in V both undergo loss in electron densities.

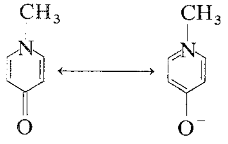

Va Vb

Acknowledgements. Most of the work presented here was supported by Public Health Grant Service Fellowship No. 1-F2-GM-30-752-01 and done at the Centre during 1966. The author wishes to thank the warm hospitality of Professor R. Daudel and the aid of Drs. O. Chalvet, G. Bessis, P. Kottis, and C. Moser. In addition, the author thanks both CNRS and the Faculty Research Committee of the University of California at Santa Cruz.

References

1. Kubota, T.: J. chem. Soc. Japan **79**, 930 (1958); **80**, 578 (1959).
2. — Bull. chem. Soc. Japan **35**, 946 (1962).
3. Ito, M., and N. Hata: Bull. chem. Soc. Japan **28**, 260 (1955).
4. —, and W. Mizushima: J. chem. Physics **24**, 495 (1956).
5. Jaffé, H. H., and M. Orchin: Theory and applications of ultraviolet spectroscopy, pp. 381—383. New York: John Wiley and Sons, Inc. 1962.
6. Sidman, J.: Chem. Rev. **58**, 689 (1958).
7. Murrell, J. N.: Theory of the electronic spectra of organic molecules, p. 188. London: Methuen and Co., Ltd. 1963.
8. Ziolkowsky, B., and F. Dörr: Ber. Bunsenges. physikal. Chem. **69**, 448 (1965).
9. Saison, R., and H. H. Jaffé: Compt. Rend. **257**, 667 (1963).
10. Pariser, R., and R. G. Parr: J. chem. Physics **21**, 446, 767 (1953).

11. Pople, J. A.: Trans. Faraday Soc. **49**, 1375 (1953).
12. Parr, R. G.: J. chem. Physics **33**, 1184 (1960).
13. Sandorfy, C.: Electronic spectra and quantum chemistry, p. 108. Cliffs, N. J.: Englewood Prentice-Hall, Inc. 1964.
14. Evleth, E. M.: unpublished results.
15. Gardner, J. N., and A. R. Katritzky: J. chem. Soc. (London) 4375 (1957).
16. Hinze, J., and H. H. Jaffé: J. Am. chem. Soc. **84**, 540 (1962).
17. Stevenson, P. E.: J. mol. Spectroscopy **15**, 220 (1965).
18. Petruska, J.: J. chem. Physics **34**, 1120 (1961).
19. Reference 4, Chapter 12.
20. Evleth, E. M., and R. J. Cox: J. physical Chem. **71**, 4082 (1967).
21. Godfrey, M., and J. N. Murrell: Proc. Roy. Soc. (London) A **278**, 57 (1964).
22. Labhart, H., and G. Wagniere: Hel. chim. Acta **46**, 1314 (1963).
23. Kosower, E. M., and P. E. Klinedinst, Jr., and J. C. Burbach: J. Am. chem. Soc. **78**, 5838 (1956).
24. Brown, R. D., and M. L. Heffernan: Austr. J. Chem. **12**, 554 (1959).
25. Mataga, S., and N. Mataga: Bull. chem. Soc. Japan **32**, 521 (1959).
26. Forster, L. S., and K. Nishimoto: Theoret. chim. Acta (Berl.) **4**, 155 (1966).
27. Berthod, H., C. Giessner-Prettre, and A. Pullman: Int. J. Quant. Chem. **1**, 123 (1967).
28. Mason, S. F.: J. chem. Soc. (London) 1253 (1959).
29. Evleth, E. M.: Studies of some heterocyclic anhydrobases: Dissertation, University of Southern California 1963, pp. 141—152.
30. Allinger, N. L., and J. C. Tai: J. Am. chem. Soc. **87**, 2081 (1965).
31. — —, and T. S. Stuart: Theoret. chim. Acta (Berl.) **8**, 101 (1967).
32. —, and T. S. Stuart: J. chem. Physics **47**, 4611 (1967).
33. Evleth, E. M.: J. chem. Physics **46**, 4151 (1967).
34. — J. Am. chem. Soc. **89**, 6445 (1967).
35. Katritzky, A. R., E. W. Randall, and L. E. Sutton: J. chem. Soc. (London) 1769 (1957).
36. Sharpe, A. N., and S. J. Walker: J. chem. Soc. (London) 4522 (1961).
37. Albert, A., and J. M. Phillips: J. chem. Soc. (London) 1294 (1956).
38. Berson, J. A., E. M. Evleth, and S. L. Manatt: J. Am. chem. Soc. **87**, 2901 (1965).
39. Clementi, E., H. Clementi, and D. R. Davis: J. chem. Physics **46**, 4725 (1967).
40. Kosower, E. M.: J. Am. chem. Soc. **80**, 3251 (1958).
41. Berson, J. A.: J. Am. chem. Soc. **75**, 521 (1953).

Dr. E. M. Evleth
Board of Studies in Chemistry
The University of California
Santa Cruz, California 95060, USA